Protein Science (1992), *1*, 892–901. Cambridge University Press. Printed in the USA.

Charge balance in the α-hydroxyacid dehydrogenase vacuole: An acid test

ANTONIO CORTES,[1] DAVID C. EMERY,[2]
DAVID J. HALSALL,[2] RICHARD M. JACKSON,[2]
ANTHONY R. CLARKE,[2] AND J. JOHN HOLBROOK[2]

[1] Department of Biochemistry and Physiology, University of Barcelona, Martí y Franqués 1, 08028 Barcelona, Spain
[2] Molecular Recognition Centre and Department of Biochemistry, University of Bristol School of Medical Sciences, University Walk, Bristol BS8 1TD, UK

(RECEIVED December 19, 1991; REVISED MANUSCRIPT RECEIVED February 25, 1992)

Abstract

The proposal that the active site vacuole of NAD$^+$-*S*-lactate dehydrogenase is unable to accommodate any imbalance in electrostatic charge was tested by genetically manipulating the cDNA coding for human muscle lactate dehydrogenase to make a protein with an aspartic acid introduced at position 140 instead of the wild-type asparagine. The Asn 140–Asp mutant enzyme has the same k_{cat} as the wild type (Asn 140) at low pH (4.5), and at higher pH the K_m for pyruvate increases 10-fold for each unit increase in pH up to pH 9. We conclude that the anion of Asp 140 is completely inactive and that it binds pyruvate with a K_m that is over 1,000 times that of the K_m of the neutral, protonated aspartic-140. Experimental results and molecular modeling studies indicate the pK_a of the active site histidine-195 in the enzyme–NADH complex is raised to greater than 10 by the presence of the anion at position 140. Energy minimization and molecular dynamics studies over 36 ps suggest that the anion at position 140 promotes the opening of and the entry of mobile solvent beneath the polypeptide loop (98–110), which normally seals off the internal active site vacuole from external bulk solvent.

Keywords: charge complementarity; human muscle isoenzyme; lactate dehydrogenase; protein engineering; site-directed mutagenesis; vacuole stability

There is considerable evidence that the form of lactate dehydrogenase (LDH) in which very fast hydride transfer takes place is one in which the substrate and the dihydronicotinamide ring of the coenzyme are trapped inside the protein in a vacuole that is only sufficiently large to accept substrates up to C4 and which can only form when the ionizing groups within the vacuole have the same total overall formal charge as is present in the wild-type enzyme complex with NAD$^+$ and lactate (Dunn et al., 1991). Some groups that determine the size of the vacuole have been identified and their putative role examined by making them smaller and obtaining an enzyme that would tolerate larger substrates (Wilks et al., 1990).

Reprint requests to: J. John Holbrook, Molecular Recognition Centre and Department of Biochemistry, University of Bristol School of Medical Sciences, University Walk, Bristol BS8 1TD, UK.

The concept that the functional vacuole has an overall charge balance of zero (summed over the substrate, coenzyme ring, and histidine-195) arose because (1) only complexes of zero overall charge were bound tightly (Parker & Holbrook, 1977; Lodola et al., 1978; Parker et al., 1978) and (2) high concentrations of either the competitive inhibitor oxamate or of a slow substrate (nitrophenylpyruvate) could drive the uptake of a proton from bulk solvent at pH 8 where histidine-195 in the complex with NADH is normally unprotonated (Holbrook, 1973). The charge balance property was used to design a malate dehydrogenase on the LDH framework, and one in which charge balance was preserved (Wilks et al., 1988) was dramatically better than one in which formal charge balance was not maintained (Clarke et al., 1987; Wilks, 1990).

There is some uncertainty about which positions must be counted as being in the vacuole and which may be con-

sidered as being on the periphery and only exert a second order ionic effect. Both distance from the hydride transfer pathway and exposure to bulk solvent should be important. Ionizing groups that are presently considered to be in the vacuole are arginine-109 (Clarke et al., 1986), arginine-171 (Hart et al., 1987), histidine-195 (Holbrook & Ingram, 1973), and aspartate-140 (this paper); see Kinemage 2 for their positions. Residues that are on the vacuole periphery, partly solvent-exposed, and whose ionization state can change without total disruption of binding or catalysis are glutamate-107 (Scawen et al., 1989), aspartate-197 (Wilks et al., 1988), and tyrosine-237 (Parker et al., 1982). One residue that is part of the catalytic pathway and forms a charge couple with histidine-195 is aspartic acid-168 (Clarke et al., 1988). Yet a neutral mutant at this position, alanine-168, while having a very large K_m is still reasonably active, albeit being now rate-limited by chemical bond breaking rather than vacuole closure. There have always been two possible interpretations of poor enzyme properties when a vacuole anion has been substituted by a nonionizing amino acid: (1) the charge-imbalanced vacuole does indeed have weak enzymic properties, and (2) a small proportion of bases (e.g., histidine-68 or lysine-243) close to the vacuole could deprotonate to preserve charge neutrality, albeit then in only a minor population of the enzyme molecules.

Rigorous tests of the charge balance requirement have not been possible with the *Bacillus stearothermophilus* LDH because this enzyme requires fructose-1,6-bisphosphate (FBP) binding at histidine-188 for full activity, and the pH dependence of K_m for substrate is complicated by the changed phosphate ester ionization in FBP and histidine-188 ionization in a range above pH 6. For these reasons we have had to develop mutagenesis in a cloned, overexpressed human muscle M_4 LDH (Kinemage 1; Barstow et al., 1990), which is not regulated by FBP and which has simple binding versus pH curves (Holbrook & Stinson, 1973) to rigorously test whether charge-imbalanced LDH active site vacuoles can have even weak enzyme activity. By inserting an aspartic acid instead of asparagine-140, a residue that normally forms a hydrogen bond to the substrate carbonyl-oxygen, we show that no charged-imbalanced complexes form and that no enzyme activity exists at levels above 1/1,000 of that of the charge-balanced complexes. This is a rigorous test of the requirement for charge balance in the active center vacuole.

Results and discussion

To test the proposal that the LDH was inactive with imbalanced charge within the catalytic vacuole a new negative charge (at pH > 5) was deliberately inserted into the catalytic vacuole by using the polymerase chain reaction (PCR) to mutate the asparagine-140, which forms a hydrogen bond to the substrate carbonyl (Fig. 1) to an aspartate. This is the first site-directed mutation of a mesophilic, eukaryote LDH we have obtained. The steady-state enzyme kinetics of this mutant showed it to have very low activity at pH 6 because the $K_{m\text{apparent}}$ for pyruvate was increased to 150 mM with unchanged k_{cat} (335 s^{-1}). With many mutant LDHs (Wilks et al., 1988, 1990; Dunn et al., 1991) poor enzyme activity results from a great slowing of the chemistry of hydride transfer so that, unlike the wild-type enzyme, which is rate-limited by a conformation change, the mutants become rate-limited by hydride transfer. The diagnostic for hydride transfer limitation is that the rate at saturating (nicotinamide-4-^{2}H) NADD is 2–4 times slower than with NADH. In the present case the primary deuterium kinetic isotope ratio was close to 1.1, both for the wild type and the mutant. This suggested that the rate of the N140D mutant was limited by the normal conformation change of the protein but that only a very small proportion of the molecules was in an active state at pH 6.

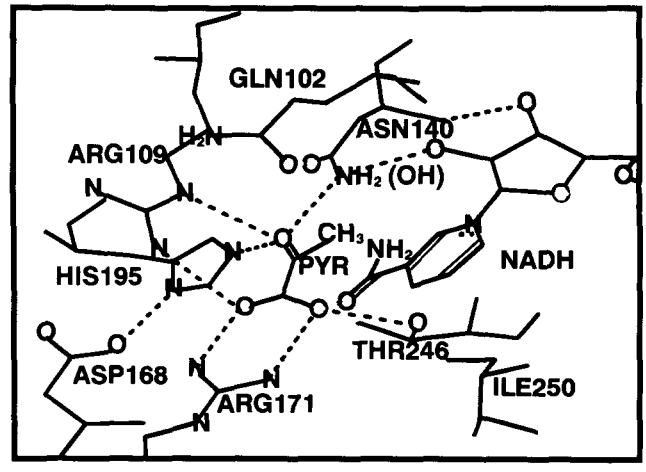

Fig. 1. The groups that surround the catalytic pathway in the X-ray structure of pig M_4 LDH. The coordinates are from Dunn et al. (1991) for the structure of the pig M_4 LDH–NADH–oxamate complex. The NH_2 of oxamate was replaced by the isoelectronic and isosteric CH_3 of pyruvate. Dotted lines are donor and acceptor pairs at the correct distance to form hydrogen bonds. The residues shown are identical in dogfish and pig M_4 LDH and in *B. stearothermophilus* LDH. Asn 140 was the residue changed to aspartate to test the tolerance of the vacuole to imbalanced charge.

To test this conclusion the pH dependence of velocity (under conditions of constant $[S] < K_m$, such that $v_0 = V_{max} \cdot [S]/K_{m\text{app.}}$) was measured between pH 4 and pH 9. This curve is shown as Figure 2. Under these conditions the rate/pH curve reports the variation in apparent K_m with pH. For the unmodified human enzyme this shows the expected pK_a at about pH 7, which reflects the requirement for the protonation of histide-195 seen in all LDHs (Holbrook & Stinson, 1973; Holbrook et al., 1975). The same K_m curve for the Asp 140 mutant enzyme is on a plateau below pH 4.5 and increases 10-fold for each pH increase of 1 above pH 5 up to the limit of measurement

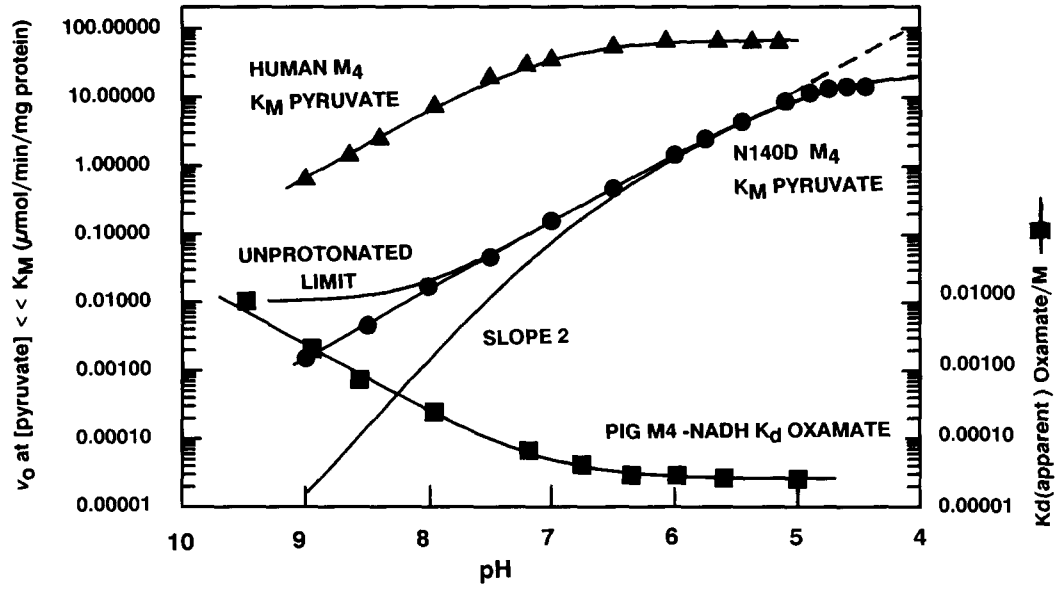

Fig. 2. The pH dependence of pyruvate binding to wild-type (M_4) human LDH (Asn 140) and its Asp 140 mutant. The buffers were 0.1 M citrate-0.2 M phosphate (pH 4-8), 0.1 M Tris (pH 7.5-9.0). [Pyruvate] was 10 μM (wild type) or 0.35 mM (mutant). Initial velocities (left hand axis) are μmol/min/mg determined in triplicate for wild type (—▲—) or for the D140 mutant (—●—). No loss of enzyme activity was observed at pH ≥4.5. At this pH $-A_{340}$/min due to NADH decomposition was <5% of the enzyme-catalyzed rate, and progress curves were linear. A complete measure of k_{cat} and K_m at pH 4.5 gave k_{cat} = 300 s^{-1}, $K_{m(apparent)}$ = 10 mM. The pH-$K_{d(oxamate)}$ (—■—) for pig M_4 NADH-oxamate results (right-hand axis) are replotted from Holbrook and Stinson (1973) and are modeled by an acid K_d limit of 28 μM and pK_a = 7. The K_m of human M_4 enzyme for pyruvate is modeled also by pK_a = 7. The slope 2 curve models the situation where both Asp 140 and His 195 (pK_a = 7) must be protonated in a functional complex. The unprotonated limit curve models the situation where the anion of Asp 140 is active with K_m 10,000 times greater than that of the protonated acid. The model of Figure 3 predicts a linear change in v_0 (K_m) for pyruvate for the Asp 140 mutant from pH 9 to pH 4.

at pH 9. This monotonic decrease shows that pyruvate will not bind in either an active or inactive state to the enzyme-NADH complex containing ionized aspartate-140. Substrate is only reduced when a group with pK_a < 4 is protonated. The K_m is ≤ 3 mM at pH 4. We first thought the group responsible for the plateau at pH 4 was protonated aspartic acid. Indeed, other values measured in Table 1 show that interpretation of these results in terms of the protonation state of Asp 140 is reasonable and allows neglect of possible changed binding of NADH.

Table 1 shows that the $K_{d(NADH)}$ was unaltered by the mutation. Both the K_i for a strict competitive inhibitor (oxamate) and the K_d oxamate from enzyme-NADH were increased to the same extent by the mutation as was the K_m for pyruvate. The K_d for this complex was also increased by the mutation in the same way as the K_m for pyruvate. At pH 4.5 the k_{cat} and K_m for pyruvate could still be measured under conditions where the rate of decomposition of NADH was small compared to the enzyme rate. This curve showed, as expected from the interpretation of the curve of Figure 2, that k_{cat} was unchanged at 300 s^{-1} but that K_m had decreased to about 10 mM. Technically, it was necessary to work at 0.125 μM Asp 140 enzyme subunits, because at lower enzyme concentrations the progress curves started to slow with time, indicating that irreversible denaturation was occurring in the assay cuvette. Muscle LDH readily dissociated from a stable tetramer to unstable monomer in acid. Oxalate forms a complex with unprotonated His 195 enzyme-NAD^+ and as expected from the required charge balance in the vacuole, its K_i is also much increased by the mutation.

The mechanism of Figure 3 was used to model the effects of certain mechanistic assumptions. (1) Assume that it was possible for there to be activity with the anionic form of Asp 140 but with a K_m increased to 0.01 M. This assumption predicts the linear decrease in rate with increased pH with a plateau at an unprotonated limit above pH 8. No such limit is visible in the experimental results, and we conclude that such activity or binding must be less than 1/1,000 of that of the unprotonated Asp 140. (2) Assume that the pK_a of His 195 remains at 7 (its value in the binary complex [Holbrook & Ingram, 1973]) and that in the mutant containing Asp 140 both groups must be protonated to maintain charge balance and activity. This predicts that starting from pH 6 the decrease in rate would be 100-fold for each increase in pH of 1, a slope of 2 on Figure 2. There is no evidence of such limit appearing up to pH 9. We thus conclude that in the presence of Asp 140 the pK_a of His 195 is raised to greater than 9. It is likely that the pK_a of His 195 would be increased by the nearby anion at position 140.

Table 1. *Kinetic and binding properties of wild-type human (M_4) LDH and the Asp 140 mutant*

Constant	Wild type (Asn 140)	Mutant (Asp 140)
pH 6.0		
k_{cat} (s^{-1})[a]	350	335
$K_{m(pyruvate)}$ (mM)[a]	0.08	150
$K_{i(oxamate)}$ (mM)[a]	0.02	43
$K_{i(oxalate)}$ (mM)[a]	0.014	40
$K_{d(NADH)}$ (μM)[b]	1.2	1.1
$K_{d(oxamate)}$ (mM)[c]	0.018	37
k_H/k_D	1.15[d]	n.d.[e]
	1.2[f]	1.15[f]
pH 4.5		
k_{cat} (s^{-1})[g]	n.d.	300
$K_{m(pyruvate)}$ (mM)[g]	n.d.	≈10

[a] Steady-state values with [pyruvate] 0.04–0.4 mM (wild type) and 4–40 mM (Asp 140) mutant enzyme 2.7 nM subunits, NADH (0.15 mM). Oxamate (0.01–0.04 mM [wild type] and 20–80 mM [for the Asp 140 mutant]) is a competitive inhibitor of pyruvate and K_i is the K_d of the LDH-NADH-oxamate complex. Oxalate at the same concentrations is an uncompetitive inhibitor and the K_i is a complex constant.

[b] Obtained fluorimetrically with 6 μM NADH.

[c] Obtained fluorimetrically with 12 μM subunits and 10 μM NADH.

[d] Primary deuterium kinetic isotope effects were from single turnover experiments.

[e] n.d., not determined.

[f] The mutant has high $K_{m(pyruvate)}$ and its primary kinetic isotope ratio could only be deduced from steady-state measurements of k_{cat}.

[g] Steady-state values with [pyruvate] 0.1–5 mM, [NADH] = 0.15 mM, 0.125 μM (subunits) Asp 140 mutant enzyme.

Because bringing two acids together normally increases the acidity of the more acidic and decreases that of the weaker acid, this suggests that increasing the pK_a of His 195 by over 3 units (say to 10) results in the pK_a of Asp 140 decreasing from its expected value of 3.5 to 0.5. This analysis demonstrates that the apparent pK_a of 4.5 shown in Figure 2 is not the intrinsic pK_a of Asp 140 (a point confirmed by modeling—see below).

Ionized aspartate-53 facilitates the distinction between NAD^+ and $NADP^+$ (Feeney et al., 1990). The measurements of Figure 2 were made at 0.2 mM NADH, some 20 times the K_m (NADH). However, because the LDH mechanism involves compulsory order of addition of coenzyme followed by substrate, any increase in K_m for NADH above 0.2 mM could lead to an apparent plateau in Figure 2 (Holbrook et al., 1975). The experimental results of Fawcett and Kaplan (1962) indicate that the pK_a of the acid controlling the NADH/NADPH discrimination is much less than 5 and thus an unlikely explanation for the pH 4 plateau.

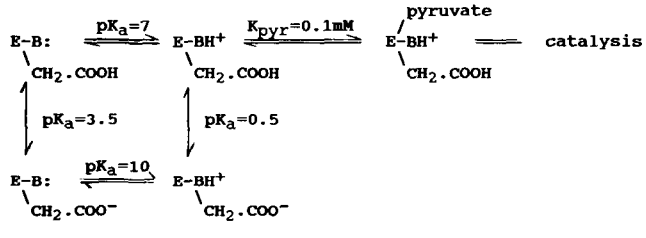

Fig. 3. Model for the effect of the nearby charge of Asp 140 on the pK_a of His 195 in the vacuole of LDHs. As with Figure 2, only a complex with protonated His 195 and protonated Asp 140 is active and able to catalyze hydride transfer. The pK_a of His 195 with Asp 140 ionized was calculated (Table 2) from modeling to be ≥10. B: is His 195; $-CH_2 \cdot COOH$ is Asp 140. All complexes contain NADH.

Calculated shift in the pKa of His 195 due to the effect of the Asn 140–Asp mutation

The calculated change in pK_a of His 195 for two different conformations of the aspartate side chain (crystal and model-built) are given in Table 2. The effect of neglecting the contribution of asparagine in the calculation of ΔpK_a and the dependence of the calculations on the partial charge distribution are also assessed. The model predicts that introduction of an aspartate residue at 140 will cause a significant positive shift in the macroscopic pK_a of histidine ($6 > \Delta pK_a > 1.3$). The calculations predict that deprotonation of His 195 is unlikely within the pH range of the enzyme assays (4–9). However, the aspartate side chain conformation creates a very large uncertainty in the His pK_a. The neglect of charge distribution on Asn 140 strongly influences the lower limit of ΔpK_a,

Table 2. *Calculated shift in the pK_a of His 195 due to the effect of the Asn 140–Asp mutation*[a]

	ΔpK_a	
Model	Crystal	Conf-II
I	7.07	2.01[b]
II	6.31	1.25
III	6.77	1.26

[a] Two extreme conformational states for the aspartate side chain were analyzed. Crystal corresponds to the observed conformation of asparagine-140 in the apoenzyme crystal structure and Conf-II to a model-built structure in which the side chain was rotated away from His 195 as far as was sterically reasonable, leaving the side chain torsion angle (χ1) in a gauche$^+$ conformation. The inclusion of the potential generated by histidine at asparagine-140 ϕasn was deemed important as the closest approach of heavy atoms for the two residues in the crystal structure is 4.2 Å. Thus, model I was calculated from the difference in potential generated at all atoms on Asn and Asp for the united atom Biosym charge set ($\Delta pK_a = \Sigma\, q_i[\phi asn_i - \phi asp_i]/2.303$). Model II is the same as above; however, it neglects the contribution of asparagine ($\Delta pK_a = \Sigma\, q_i[-\phi asp_i]/2.303$). In Model III only the side chain carboxyl oxygens are considered charged with a value of −0.5e on either oxygen, whereas the contribution of Asn is neglected ($\Delta pK_a = \Sigma\, q_i[-\phi asp_i]/2.303$). *Note*: All values of ΔpK_a are positive, leading to an increase in the histidine pK_a. Asp 140 is fixed in the conformation of Asn 140 in the crystal structure.

[b] Asp 140 with a conformation of the minimized model-built structure.

whereas partial charge distribution on Asp 140 has much less effect.

The results were somewhat dependent on grid size, with the results for the two finest grid sizes differing by about 10%. However they were less dependent on rotational averaging (Gilson et al., 1987) at the finest grid spacing. The results of four runs on the finest grid spacing using rotational averaging varied from the mean value of ΔpK_a by less than 2% when using the coordinates of enzyme crystal structure (which had the largest ΔpK_a dependence on grid orientation and during focusing).

If the anion of Asp 140 continually becomes more protonated as pH is decreased to <4 then why does the curve of Figure 2 plateau at pH 4? A likely explanation is that only a minute fraction of the other acids in the LDH vacuole are protonated above pH 5, and the amount is not sufficient to disrupt charge balance and influence the apparently monotonic pH dependence from pH 5 to 9. However, at below pH 5, there will begin to be an appreciable fraction of the glutamic and aspartic acids, for example Glu 107 (Scawen et al., 1989), Asp 197 (Clarke et al., 1987), Glu 194 and Asp 168 (Clarke et al., 1988), which line the vacuole in a protonated state (assuming they have standard pK_a values). If these acids are required to be unprotonated to achieve charge balance, then protonating them will result at first in a maximum and then a decrease in activity below pH 4. The optimum and decrease are experimentally inaccessible, as irreversible denaturation of the protein and NADH decomposition become very rapid below pH 4.

Calculated effect of Asn 140–Asp mutation on the free energy of binding pyruvate

The difference in electrostatic free energy of binding pyruvate in the mutant ternary complexes for both the apo (loop up) and ternary (loop down) enzyme conformations are given in Table 3. The protonated form of aspartate has a negligible effect on $\Delta(\Delta G_{bind})$. It is predicted to slightly enhance the enzyme's affinity for pyruvate, i.e., to be slightly better than Asn 140. The negatively charged aspartate species is predicted to abolish substrate binding in the catalytically competent loop down ternary complex. These calculations suggest that only the protonated form of the Asp 140 enzyme is a kinetically significant species. This was also the experimental result.

Table 3. *Calculated effect of Asn 140–Asp mutation on the free energy of binding pyruvate*

	$\Delta(\Delta G_{bind})$[a] (kcal/mol)	
Mutation	Apo-crystal	Ternary-crystal
Asn 140–Asph	n.d.[b]	−1.53
Asn 140–Asp$^-$	8.96	29.49

[a] $\Delta(\Delta G_{bind}) = \Sigma\, q_i(\phi asp_i - \phi asn_i)$ for the united atom Biosym charge set. Asph and Asp$^-$ are the protonated and anionic form of aspartic acid-140.
[b] n.d., not determined.

The active site loop conformation has some effect on the enzyme's affinity for pyruvate, $\Delta(\Delta G_{bind})$ being three times more unfavorable in the loop closed conformation than in the loop open conformation. The value of the effective dielectric constant (ϵ_{eff}) calculated from a simple Coulomb's law approximation (for the interaction of two point charges of given separation) indicates that ϵ_{eff} is reduced by a factor of three upon closure of the active site loop. Thus loop closure involving removal of bulk solvent from active site residues brings about a dramatic increase in the importance of electrostatic interactions in the active site vacuole. However, to view this region as a low dielectric medium is clearly not helpful, as the internalized active site is a highly polar environment composed of acidic and basic groups involved in ion-pair interactions. Internalization of polar active site residues clearly serves to increase the importance of charge conservation, albeit in a polar environment (Yadav et al., 1991).

The large positive value of ϵ_{eff} will clearly have consequences for the conformational viability of the charged mutant ternary complex. It has been noted by Warshel and Russell (1984) that the upper limit of protein stabilization for a repulsive charge interaction cannot exceed the folding energy of the protein (which is on the order of 15 kcal/mol [Smith et al., 1991]) otherwise the protein will undergo local denaturation. Because the charged form of the mutant loop down ternary complex is destabilized by about 30 kcal/mol over wild type, it was predicted there would be local unfolding if the system was treated as a dynamic entity. This conclusion was tested by the use of molecular dynamics, which allows the active site to move toward an energetic equilibrium. A dynamics and energy-minimized model of the *B. stearothermophilus* LDH vacuole has already been constructed and shown to behave in accord with experiment (Clarke et al., 1991).

Molecular dynamics study

The results in Table 4 show that only the active site loop moves to a significant extent following energy minimization and molecular dynamics for 35 ps. Both wild-type and the mutant enzymes move, with the structure of post-dynamics main chain backbone atoms having a root mean square (rms) difference from the crystal structure of between 1.1 and 1.5 Å for the large loop (residues 101–121) and 0.52 and 0.5 Å for all other residues. The main quantitative difference in loop motion comes between the tip of the loop (residues 103–109) in the wild-type enzyme (1.85 Å) and the two mutant models (2.36 and

Table 4. *The rms fit of backbone atoms (N, CA, C, O) of crystal structure with the initial minimized (min) structure and the minimized structure following 35 ps dynamics (dyn)*

	Wild type		Model I[a]		Model II[b]	
Region	Min	Dyn	Min	Dyn	Min	Dyn
All[c]	0.56	0.66	0.55	0.72	0.58	0.71
Stable[d]	0.49	0.55	0.46	0.52	0.53	0.53
Large loop[e]	0.89	1.15	0.94	1.63	0.82	1.51
Small loop[f]	1.34	1.85	1.34	2.95	1.06	2.36

[a] Model I refers to the Asp 140 structure in which the system has overall net negative charge (see Materials and methods).

[b] Model II refers to the Asp 140 structure in which Asp 197 is considered charge neutral and the system has an overall neutral charge.

[c] All corresponds to all mobile residues in the simulation.

[d] Stable corresponds to all mobile residues with the exception of loop residues 101–121.

[e] Large loop corresponds to residues 101–121.

[f] Small loop corresponds to residues that constitute the active site loop "tip" (103–109).

2.95 Å). The residues Asn 102 and Arg 109 of the loop tip project into the active site vacuole, and hence this region, which is known to have a high degree of conformational flexibility, will be most sensitive to changes in the active site environment. In the crystal structure of *B. stearothermophilus* the loop is less closely packed down on the surface of the enzyme than in other LDH crystal ternary complexes (Wigley et al., 1992). It was found that on minimization of the crystal structure that the loop and remainder of the protein formed a more close packed interface. This occurred in both wild-type and mutant complexes. However, following dynamics it became evident that whereas the wild-type enzyme loop tip retained the residue–residue interactions and conformation of the minimized structure (rms of 0.91 Å), the mutant models drift away from their minimized starting conformations (rms of 1.659 and 2.427 Å for model II and model I, respectively), illustrating that the mutant complexes deviate to a much larger degree during the time of the dynamics simulation. Visual inspection of the superimposed loop structures (Fig. 4; Kinemage 3) shows that for the two mutant complexes there is a net translation of the loop tip away from the crystal conformation resulting in new contacts between residues in the loop tip and the rest of the protein. These contacts are not seen in the crystal structure or in the wild-type enzyme following dynamics. As might be expected, the conformational changes were greatest in the mutant model, which has a net charge imbalance in the active site. One external water molecule penetrates the active site to form a hydrogen bond to Asp 140, the side chain of which undergoes significant perturbation from the crystal conformation of Asn 140 to a position more closely associated with the bulk solvent. Thus again the modeling gives an explanation for the experimental result that the enzyme has high K_m at pH where residue 140 is mainly the charged aspartate.

These calculations were performed in order to access the stability of the active site conformation in the wild-type and mutant Asn 140–Asp ternary complexes. Although the simulations were of relatively short duration, it is evident that while the wild-type complex retained the essential conformational and bonding characteristics of the crystal structure, the mutant enzyme complexes showed concerted movements away from the crystal structure leading to new active site loop conformations and in one case to solvent penetration into the active site. Thus molecular dynamics provides further support for the experimental observation that the charged mutant enzyme ternary complex is energetically unstable and suggests that instability is due to the charge imbalance

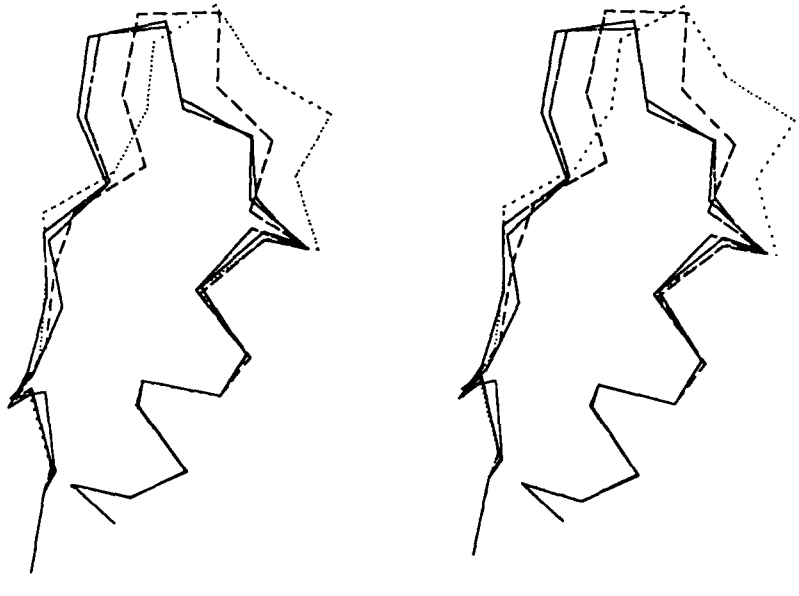

Fig. 4. The effect of charge imbalance on the structure of the active site loop (between αD and βD). Four loop structures are shown: the wild type after energy minimization of the crystal structure conformation (——); the wild type after 36 ps of molecular dynamics (– – –); model I after similar dynamics (· · · · ·); model II after similar dynamics (– – – –). Models are defined in the legend to Table 4.

forcing open the mobile loop that normally covers the active site vacuole in ternary complexes of the enzyme.

Materials and methods

Site-directed mutagenesis

The mutant protein with aspartic acid at position 140 was generated by the PCR-based overlap extension method (Higuchi et al., 1988; Ho et al., 1989). The template used was the plasmid pHLDHA22 (Barstow et al., 1990), which consists of an *Eco*RI-*Sma*I DNA fragment containing the entire human A_4 LDH coding region together with a 60-bp fragment containing the transcriptional and translational signals of the *B. stearothermophilus* LDH inserted into the expression vector pKK223-3 (Pharmacia LKB Biotechnology, Milton Keynes, UK). The conditions used to generate two overlapping fragments were identical: 100 ng of template DNA; 50 mM KCl; 10 mM Tris, pH 8.3; 1.5 mM $MgCl_2$; 0.01% w/v gelatin; 200 μM each dNTP; 1 μM of each primer; 2.5 units TAQ DNA polymerase (Perkin Elmer Cetus) in a final volume of 50 μl. Each reaction was subjected to 10 cycles of PCR with the following parameters (A): 1 min 30 s at 94 °C, 2 min at 57 °C, 2 min at 72 °C in a Perkin Elmer thermal cycler. In one reaction the antisense mutant primer (25-mer) was used in combination with the 5′-flanking primer (20-mer) specific to the *tac* promoter. In a second reaction the "sense" mutant primer was used in combination with the 3′-flanking primer (20-mer) specific to the 5S region of pKK223-3. The sequences of these oligonucleotides are listed in Table 5.

Each fragment was then separated from excess primers and template DNA by agarose gel electrophoresis using UltraPure low melting point agarose (BRL, Gaithersburg, Maryland). Each purified fragment (50 ng) was added to a single PCR reaction and subjected to five cycles of annealing and extension in the absence of primers (1 min 94 °C, 1 min at 45 °C, heat to 72 °C in 2 min, 1 min 72 °C). Flanking primers were then added and full-length product amplified for 25 cycles with parameters (A) above. The full-length product was purified by ethanol precipitation and digested with *Sma*I and *Eco*RI prior to subcloning into similarly cut pKK223-3 thus forming plasmid pHLDHAacid. The ligation products were microdialyzed and transformed into *Escherichia coli* TG2 cells made competent by electroporation. LDH overexpression in ampicillin-resistant colonies was identified from an M_r = 33,000 band appearing in sodium dodecyl sulfate (SDS)-polyacrylamide gel electrophoresis (Pharmacia Phast system). The entire coding region from an overexpressing candidate clone was resequenced using a DuPont Genesis 2000 automated sequencing system and showed only the required change.

Table 5. *Oligonucleotides used in the PCR-based overlap extension method of mutagenesis*[a]

	IleValSerAsnProValAsp
Human A_4 LDH wild-type sequence	5′-TTATTGTTTCAAATCCAGTGGATAT-3′
Human A_4 LDH sense primer	5′-TTATTGTTTCAGATCCAGTGGATAT-3′
Human A_4 LDH antisense primer	3′-AATAACAAAGTCTAGGTCACCTATA-5′
	IleValSerAspProValAsp
pKK223-3 flanking primer to tac	5′-AGCGGATAACAATTTCACAC-3′
pKK223-3 flanking primer to 5S	5′-GGGATCCGTCGACCTGCAGC-3′

[a] Double-standard DNA was obtained by mixing complementary sense and antisense single-stranded DNA. The sense strand was amplified off the wild-type gene between a mutant sense primer and a primer to the 5S region of pKK223-3. The antisense strand was amplified with a primer flanking the *tac* promoter region of the vector pKK223-3 (see text for details).

Enzyme purifications

The wild-type human M_4 LDH was purified as described by Barstow et al. (1990). The N140D mutant did not bind to oxamate-Sepharose at pH 6 and required a different purification. The cells were grown up in NZCYM broth (1 L). A crude cell extract was obtained by sonication; soluble protein was precipitated with 65% $(NH_4)_2SO_4$ and dialyzed against 25 mM triethanolamine hydrochloride (TEA) buffer, pH 7, with charcoal outside the bag as described by Barstow et al. (1990). The dialysate was applied to a 1.6 × 20-cm column of Q-Sepharose Fast Flow equilibrated with the above buffer. Human LDH was not retained, but the *E. coli* LDH was. The separation of the *E. coli* and human LDHs was checked by isoelectric focusing on a pH 3–9 gel with lactate/NAD^+ formazan staining for enzyme activity (Fine & Costello, 1963). The LDH in the breakthrough peak was recovered by precipitation with 65% $(NH_4)_2SO_4$, desalted on a Sephadex G-25 column in 20 mM Na phosphate, pH 6.8, and applied to a 1.6 × 20-cm column of S-Sepharose in the same buffer and was eluted in a linear gradient (0–0.5 M) of NaCl at about 0.1 M NaCl. The enzyme was estimated to be >98% pure from the Coomassie blue stain of both SDS-polyacrylamide and pH 3–9 isoelectric focusing gels run in a Pharmacia Phast system. Protein was estimated from $A_{280\,nm}$ = 1.2 for 1 mg/ml protein derived from the Trp and Tyr contents of the protein sequence. The cloned human enzyme is identical to the authentic enzyme isolated from human tissue except that the N-terminal alanine is not acetylated (Barstow et al., 1990).

Steady-state kinetics

Assays were monitored from $-A_{340\,nm}$/min at 25 °C in 67 mM Na phosphate buffer pH 6. Kinetic parameters k_{cat}, $K_{m(pyruvate)}$, $K_{i(oxamate)}$, and $K_{i(oxalate)}$ were determined at saturation with NADH (0.15 mM), and initial rates were fitted using a nonlinear regression (Leatherbarrow, 1990) to the appropriate rate equation (Cleland, 1963). The pH dependence of pyruvate binding to LDH was measured in 0.1 M citric acid and 0.2.M phosphoric acid brought to a pH in the range 4–9 with 10 M NaOH.

To obtain the pH dependence of K_m, the variation of LDH activity with pH was obtained at [pyruvate] < K_m, where $v_0 = k_{cat} \cdot$ [pyruvate]$/K_m$ (see legend to Fig. 2). To maintain this condition the rates with the wild-type enzyme were obtained in a rapid mixing spectrometer.

Primary kinetic isotope ratios

Deuterium effects on k_{cat} were measured during a single turnover in a Hi-Tech stopped flow spectrometer SF-51 by comparing rates of $-A_{340\,nm}$ when 72 μM of either NADH or NADD and 80 μM enzyme subunits (M_r 33,000) in 67 mM Na phosphate buffer, pH 6, was rapidly mixed with 20 mM pyruvate.

Binding studies

The dissociation constants of enzyme-NADH and of oxamate from enzyme-NADH-oxamate were measured from the enhanced fluorescence of NADH or its quench by oxamate. Excitation was at 340 nm and emission at 450 nm in an SLM8000 spectrofluorimeter (SLM Instruments, Urbana, Illinois). The buffer was 67 mM Na phosphate, pH 6. For the binary complex, concentrated enzyme was continuously added to 6 μM NADH (fluorescence enhancement). For the ternary complex, concentrated oxamate was continuously added to 12 μM LDH and 10 μM NADH. The titration curves were fitted by a nonlinear regression, which corrected for the condition $[NADH]_{total}$ does not equal $[NADH]_{free}$.

Effect of Asn 140-Asp mutation on the pK_a of the active-site histidine-195 in the enzyme-NADH binary complex

To estimate the electrostatic effect of the Asn 140-Asp mutation on the pK_a of the active site His 195 we used numerical solution of the Poisson-Boltzmann equation (Klapper et al., 1986; Gilson & Honig, 1988) to calculate the electrostatic potential (ϕ) generated at reside 140 due to the charge on His 195. The atoms of both Asp 140 and Asn 140 were defined explicitly, and the potential at either residue was therefore calculated in separate runs. ΔpK_a can be calculated from $\sum q_i(\phi asn_i - \phi asp_i)/2.303$.

The high resolution coordinates of the dogfish apoenzyme (Abad-Zapatero et al., 1987) were used. The coenzyme was docked into the apostructure to generate the enzyme-NADH binary complex, in accordance with the coenzyme conformation in the dogfish ternary complex. The following side chain torsion angles were changed to relieve bad van der Waals contacts with the coenzyme; Val 31(χ1), Asp 52(χ1, χ2), Met 54(χ1, χ2, χ3), Thr 95(χ1), Thr 245(χ1), and Ile 241(χ1, χ2). In all cases torsion angles were changed to adopt the conformation observed in the ternary crystal structure as closely as was possible.

Effect of Asn 140-Asp mutation on the pyruvate binding in the enzyme-NADH-pyruvate ternary complex

Numerical solution of the Poisson-Boltzmann equation was used to calculate the change in electrostatic free energy of binding pyruvate due to the charge on the mutant Asp 140 in its neutral (protonated) and anionic states, in a similar manner to the approach used by Hurley et al. (1990). This approach neglects the contribution of the free energy difference between the wild-type and mutant binary enzyme complexes (the whole thermodynamic cycle should be considered in order to calculate $\Delta(\Delta G_{bind})$. Hence, the value of $\Delta(\Delta G_{bind})$ given in Table 3 is not strictly the free energy of binding. However, the inclusion of a negatively charged residue (aspartate-140) in the active site vacuole is analogous to the addition (binding) of the negatively charged substrate (albeit at a different position in the active site) and would be expected to further destabilize the binding of substrate to the mutant enzyme, i.e., the value of $\Delta(\Delta G_{bind})$ given in Table 3 would be more positive if we considered the whole thermodynamic cycle.

Two conformational states of the enzyme in the enzyme-NADH-pyruvate ternary complex were assessed. The first corresponds to a loop open ternary complex. This was generated from the binary complex (see above) by docking pyruvate into the active site to reproduce its observed binding mode in the ternary enzyme crystal. Docking required only minimal adjustment of the side chain torsion angles of Arg 171 and His 195 (to adopt their observed conformations of the ternary crystal complex). The carboxyl group of the substrate can form a bifurcated ion-pair interaction with Arg 171 while maintaining a hydrogen bond with the side chain hydroxyl group (OG1) of Thr 246. Furthermore, the substrate carbonyl oxygen can hydrogen bond to the protonated NE2 of His 195. Thus all the direct hydrogen bonds except those of Arg 109 to the substrate seen in the enzyme (loop down) ternary crystal can be satisfied in the loop open model built ternary complex. The second enzyme conformation corresponds to the loop down state, for which the high resolution coordinates of the dogfish ternary complex were used.

Models and parameters

The linearized Poisson-Boltzmann equation was solved using the program DELPHI (Biosym Technologies) run on a Silicon Graphics Personal IRIS 4D-20 workstation. The enzyme, NADH, and pyruvate were considered as low-dielectric regions surrounded by high dielectric solvent. The molecular dielectric (ϵ_m) was set at 2, and the solvent dielectric (ϵ_s) was that of water (80) (Sharp & Honig, 1990). However, because we were unable to experimentally quantify ΔpK_a or $\Delta(\Delta G_{bind})$ it was unnecessary to calculate the dependence of the results on the

molecular dielectric (ϵ_m). The parameter set of the united atom consistent valence force field (CVFF) (Dauber-Osguthorpe et al., 1988) provided the charges for histidine, asparagine, and both protonated and deprotonated aspartate-140. The united atom force field, which defines polar hydrogens explicitly, was used to define the shape of the low dielectric regions, and hydrogen, nitrogen, and oxygen were given radii of 1.2 Å, 1.5 Å, and 1.6 Å, respectively (Spedding & Gsneidner, 1975). The ionic strength of the phosphate/citrate buffer used for the enzyme assays was used in the calculation (0.15 M) in addition to an ion exclusion layer of 2.0 Å (determined from the average ionic radii of phosphate buffer). Certain enzyme assays were carried out in citrate buffer; however, this is expected to have little influence on the results, given the small difference in the radii of a phosphate and carboxylate.

In the enzyme binary complex, potentials generated at Asn and Asp 140 due to the charge on histidine-195 were calculated using a three-step focusing procedure: with the first calculation using a 2.90-Å grid spacing and a Coulombic boundary approximation, followed by two successive focusing calculations using grids of 0.89 Å and 0.53 Å.

In the enzyme ternary complex, potentials generated at pyruvate due to the charge on Asn and Asp 140 (in its protonated and charged states) were calculated using a two-step focusing procedure using grids with 2.90-Å and 0.89-Å spacings. The three-step focusing was unnecessary due to a difference of less than 10% in ΔpK_a between the first and second focusing runs in the previous calculations.

Dynamics and energy minimization

Simulations were based upon the high resolution coordinates of *B. stearothermophilus* LDH in a loop down ternary complex with NADH and oxamate (Wigley et al., 1992). A fixed boundary method was used with a 15-Å reaction zone centered at the carbonyl carbon of oxamate with a 3-Å fixed buffer region and water molecules filling nonprotein regions within the 15-Å reaction zone. Within this zone the sequences of both the eukaryote and prokaryote LDH are highly conserved, right down to the position of the "frozen" (low B-value) waters, which are thought to order the seven H-bonds from protein to substrate (Dunn et al., 1991; Wigley et al., 1992). Initial conformations for the simulation were generated by changing the NH_2 of oxamate to CH_3 to generate pyruvate. The mutant complex was generated from this model by changing Asn 140 to Asp leaving the side chain torsion angles unchanged. The protein, coenzyme, and pyruvate were all modeled using the CVFF (Dauber-Osguthorpe et al., 1988) with the exception of charges on the coenzyme and substrate. Charges on coenzyme, pyruvate, and known fragments from the CVFF library were generated using MNDO semiempirical molecular orbital calculations (Dewar & Thiel, 1979) in the program MOPAC version 4.0. A best fit scaling factor, which made the charges of the known fragments match those of the CVFF charge library, was deduced using several charged and uncharged species. This scale factor was then applied to the charges of NADH and pyruvate. A united atom model, which incorporates nonpolar hydrogens into the carbon heavy atoms, was used for amino acid residues, whereas all atom models were used for the coenzyme and substrate.

All algorithms were implemented by a vectorized version of DISCOVER 2.4 (Biosym Technologies) run on an IBM 3090-150S computer. A nonbonded cutoff of 12 Å with a switching function between 10 and 12 Å was used. The nonbonded pair list was updated every 30 cycles, and a dielectric constant of 1 was used in all calculations. Only Arg 109, Arg 171, His 195, Asp 168, Asp 197, and the substrate carboxyl group were considered charged. To this was added Asp 140 in the mutant simulation but no counter charge was added because the nearest potentially positively charged residue (Lys 103) was some 14 Å distant and in a solvent-exposed position. The incorporation of a solvent counter ion was considered; however, it cannot approach Asp 140 by more than 5–6 Å without perturbation of the active site loop conformation because Asp 140 is in a part of the catalytic vacuole inaccessible to bulk solvent. Hence the simulation represents the viability of the closed active site incorporating a negative charge at position 140. However, another simulation in which Asp 197 was considered as charge neutral was also performed, maintaining overall electroneutrality in the system. Asp 197 is partially solvent exposed but interacts with the active site Arg 109 through a water bridge. It is known that mutation of this residue to an asparagine has minimal effect on the values of k_{cat} and K_m (Wilks et al., 1988). All complexes were minimized with all protein atoms initially fixed and all waters allowed to move with the oxygen atoms lightly tethered (10 kcal $Å^{-3}$) for 200 cycles of conjugate gradients minimization. The system was further relaxed with 200 cycles of conjugate gradients with heavy atoms of the protein, coenzyme, and substrate constrained (1,000 kcal $Å^{-3}$) to crystallographic positions. This procedure allows the protein to relieve bad contacts of the added hydrogen atoms. Minimization was then continued to convergence (average derivative of <0.002 kcal/mol/Å). The resulting structures were then equilibrated at 300 °K for 4 ps and data collected for a further 32 ps using a 1-fs timestep throughout. The final structures from dynamics were then minimized as above to an average derivative of <0.002 kcal/mol/Å.

Acknowledgments

This work was supported by the Science and Engineering Research Council (UK), SmithKline Beecham Research (UK) Ltd., and The British Council (Acciones Integradas). A.C.'s sabbatical year in Bristol was supported by grant BE90-326 from

Dirección General de Investigación Cientifica y Técnica of Spain.

References

Abad-Zapatero, C., Griffith, J.P., Sussman, J.L., & Rossmann, M.G. (1987). Refined crystal structure of dogfish M4 apo-lactate dehydrogenase. *J. Mol. Biol. 198*, 445–467.

Barstow, D.A., Black, G.W., Sharman, A.F., Scawen, M.D., Atkinson, T., Li, S.S.-S., Chia, W.N., Clarke, A.R., & Holbrook, J.J. (1990). Expression of the human LDH A and B cDNAs in *E. coli*. *Biochim. Biophys. Acta 1087*, 73–79.

Clarke, A.R., Colebrook, S., Cortes, A., Emery, D.C., Halsall, D.J., Hart, K.W., Jackson, R.M., Wilks, H.M., & Holbrook, J.J. (1991). Towards the construction of a universal NAD(P)$^+$-dependent dehydrogenase: Comparative and evolutionary considerations. *Biochem. Soc. Trans. 19*, 576–581.

Clarke, A.R., Smith, C.J., Hart, K.W., Birktoft, J.J., Banaszak, L.J., Wilks, H.M., Barstow, D.A., Atkinson, T., Lee, T.V., Chia, W.N., & Holbrook, J.J. (1987). Rational construction of a 2-hydroxyacid dehydrogenase with new substrate specificity. *Biochem. Biophys. Res. Commun. 148*, 15–23.

Clarke, A.R., Wigley, D.B., Chia, W.N., Barstow, D., Atkinson, T., & Holbrook, J.J. (1986). Site-directed mutagenesis reveals the role of a mobile arginine residue in lactate dehydrogenase catalysis. *Nature 324*, 699–702.

Clarke, A.R., Wilks, H.M., Barstow, D.A., Atkinson, T., Chia, W.N., & Holbrook, J.J. (1988). An investigation of the contribution made by the carboxylate group of an active site histidine-aspartate couple to binding and catalysis in lactate dehydrogenase. *Biochemistry 27*, 1617–1622.

Cleland, W.W. (1963). The kinetics of enzyme-catalyzed reactions with two or more substrates. *Biochim. Biophys. Acta 67*, 173–187.

Dauber-Osguthorpe, P., Roberts, V.A., Osguthorpe, D.J., Wolff, J., Genest, M.G., & Hagler, A.T. (1988). Structure and energetics of ligand-binding to proteins: *E. coli* dihydrofolate reductase-trimethoprim, a drug receptor system. *Proteins Struct. Funct. Genet. 4*, 37–47.

Dewar, M.J.S. & Thiel, W.J. (1979). Ground states of molecules. 38. The MNDO method. Approximations and parameters. *J. Am. Chem. Soc. 99*, 4899–4907.

Dunn, C.R., Wilks, H.M., Halsall, D.J., Atkinson, T., Clarke, A.R., Muirhead, H., & Holbrook, J.J. (1991). Design and synthesis of new enzymes based upon the lactate dehydrogenase framework. *Philos. Trans. R. Soc. Lond. B 332*, 177–185.

Fawcett, C.B. & Kaplan, N.O. (1962). Preparation and properties of some NAD analogues with pentose and purine modifications. *J. Biol. Chem. 237*, 1709–1715.

Feeney, R., Clarke, A.R., & Holbrook, J.J. (1990). A single amino acid substitution in lactate dehydrogenases improves the catalytic efficiency with an alternative coenzyme. *Biochem. Biophys. Res. Commun. 166*, 667–672.

Fine, I.H. & Costello, L.A. (1963). The use of starch electrophoresis in dehydrogenase studies. *Methods Enzymol. 6*, 958–972.

Gilson, M. & Honig, B. (1988). Energetics of charge-charge interactions in proteins. *Proteins Struct. Funct. Genet. 3*, 32–52.

Gilson, M., Sharp, K., & Honig, B.J. (1987). Calculation of electrostatic interactions in biomolecules: Method and error assessment. *Comput. Chem. 9*, 327–335.

Hart, K.W., Clarke, A.R., Wigley, D.B., Waldman, A.D.B., Chia, W.N., Barstow, D.A., Atkinson, T., Jones, D.B., & Holbrook, J.J. (1987). A strong carboxylate-arginine interaction is important in substrate orientation and recognition in lactate dehydrogenase. *Biochim. Biophys. Acta 914*, 294–298.

Higuchi, R., Krummel, B., & Saiki, R.K. (1988). A general method of in vitro preparation and specific mutagenesis of DNA fragments. *Nucleic Acids Res. 16*, 7351–7367.

Ho, S.N., Hunt, H.D., Horton, R.M., Pullen, J.K., & Pease, L.R. (1989). Site-directed mutagenesis by overlap extension using the polymerase chain reaction. *Gene 77*, 51–59.

Holbrook, J.J. (1973). Direct measurement of proton binding to the active ternary complex of pig heart lactate dehydrogenase. *Biochem. J. 133*, 847–849.

Holbrook, J.J. & Ingram, V.A. (1973). Ionic properties of an essential histidine residue in pig heart lactate dehydrogenase. *Biochem. J. 131*, 729–738.

Holbrook, J.J., Liljas, A., Steindel, S.J., & Rossmann, M.G. (1975). Lactate dehydrogenase. *The Enzymes XIa*, 191–293.

Holbrook, J.J. & Stinson, R.A. (1973). The use of ternary complexes to study ionizations and isomerizations during catalysis by lactate dehydrogenase. *Biochem. J. 131*, 739–748.

Hurley, J.H., Dean, A.M., Sohl, J.L., Koshland, D.E., & Stroud, R.M. (1990). Regulation of an enzyme by phosphorylation at the active site. *Science 249*, 1012–1016.

Klapper, I., Hagstrom, R., Fine, R., Sharp, K., & Honig, B. (1986). Focussing of electric fields in the active site of Cu-Zn superoxide dismutase: Effects of ionic strength and amino acid modification. *Proteins Struct. Funct. Genet. 1*, 47–59.

Leatherbarrow, R.J. (1990). Grafit version 2.0. Erithracus Software Ltd., Staines, UK.

Lodola, A., Parker, D.M., Jeck, R., & Holbrook, J.J. (1978). Malate dehydrogenase of the cytosol. Ionizations of the enzyme-reduced-coenzyme complex and a comparison with lactate dehydrogenase. *Biochem. J. 173*, 597–605.

Parker, D.M. & Holbrook, J.J. (1977). An oil-water-histidine mechanism for the activation of coenzyme in the 2-hydroxyacid dehydrogenases. In *Pyridine Nucleotide-Dependent Dehydrogenases* (Sund, H., Ed.), pp. 485–495. Walter de Gruyter, New York.

Parker, D.M., Jeckel, D., & Holbrook, J.J. (1982). Slow structural changes shown by the 3-nitrotyrosine-237 residue in pig heart [Tyr(3NO_2)237] lactate dehydrogenase. *Biochem. J. 201*, 465–471.

Parker, D.M., Lodola, A., & Holbrook, J.J.(1978). Use of the sulphite adduct of nicotinamide-adenine dinucleotide to study ionizations and the kinetics of lactate dehydrogenase and malate dehydrogenase. *Biochem. J. 173*, 959–967.

Scawen, M.D., Barstow, D.A., Nichols, D.J., Atkinson, A., Clarke, A.R., Wigley, D.B., Hart, K., Chia, W.N., & Holbrook, J.J. (1989). Lactate dehydrogenase. The effects of amino acid changes on properties. In *Gesellschaft fuer Biologisches Forschung GmbH Monograph. Advances in Protein Design*, Vol. 12 (Bloecker, H., Collins, J., Schmid, R.D., & Schomburg, D., Eds.), pp. 103–115. VCH, Weinheim.

Sharp, K.A. & Honig, B. (1990). Electrostatic interactions in macromolecules. Theory and applications. *Annu. Rev. Biophys. Biophys. Chem. 19*, 301–322.

Smith, C.J., Clarke, A.R., Chia, W.N., Irons, L.I., Atkinson, T., & Holbrook, J.J. (1991). Detection and characterization of intermediates in the folding of large proteins by the use of genetically inserted tryptophan probes. *Biochemistry 30*, 1028–1036.

Spedding, F.H. & Gsneidner, H. (1975). Crystal ionic radii of the elements. In *Handbook of Chemistry and Physics*, 56th Ed. (Weast, R.C., Ed.) pp. F-198–F-200. CRC Press, Cleveland, Ohio.

Waldman, A.D.B., Hart, K.W., Clarke, A.R., Wigley, D.B., Barstow, D.A., Atkinson, T., Chia, W.N., & Holbrook, J.J. (1988). A genetically engineered single-tryptophan reporter identifies the movement of a peptide domain of lactate dehydrogenase as the event which limits the maximum enzyme velocity. *Biochem. Biophys. Res. Commun. 150*, 752–759.

Warshel, A. & Russell, S.T. (1984). Calculations of electrostatic interactions in biological systems and in solutions. *Q. Rev. Biophys. 17*, 283–422.

Wigley, D.B., Gamblin, S.J., Turkenburg, S.P., Dodson, E.J., Piontek, K., Muirhead, H., & Holbrook, J.J. (1992). The structure of a ternary complex of an allosteric lactate dehydrogenase from *B. stearothermophilus* at 2.5 Å resolution. *J. Mol. Biol. 223*, 317–335.

Wilks, H.M. (1990). Design and synthesis of new catalysts on the lactate dehydrogenase framework. Ph.D. Thesis, University of Bristol, UK.

Wilks, H.M., Halsall, D.J., Atkinson, T., Chia, W.N., Clarke, A.R., & Holbrook, J.J. (1990). Designs for a broad substrate specificity 2-hydroxyacid dehydrogenase. *Biochemistry 29*, 8587–8591.

Wilks, H.M., Hart, K.W., Feeney, R., Dunn, C.R., Muirhead, H., Chia, W.N., Barstow, D.A., Atkinson, T., Clarke, A.R., & Holbrook, J.J. (1988). A specific and highly active malate dehydrogenase by redesign of a lactate dehydrogenase framework. *Science 242*, 1541–1544.

Yadav, A., Jackson, R., Holbrook, J.J., & Warshel, A. (1991). Role of solvent reorganization energies in the catalytic activity of enzymes. *J. Am. Chem. Soc. 113*, 4800–4805.